ROZPRAWY INŻYNIERSKIE • ENGINEERING TRANSACTIONS • 24, 1, 93—117, 1976
Polska Akademia Nauk • Instytut Podstawowych Problemów Techniki

BUCKLING OF RECTANGULAR PLATES UNDER DISCONTINUOUS LOADING ALONG BOUNDARIES

JAN GOLEC (LUBLIN)

The paper deals with a problem of buckling of the elastic isotropic elastically homogeneous rectangular plates of small thickness, loaded arbitrarily along the boundaries, at the different boundary conditions assumed.

The solution presented contains two stages, i.e., 1) the determination of the distribution of the internal forces in a shield subjected to the action of the arbitrary discontinuous load and 2) the computation of the critical parameters causing the plate buckling.

In the first stage the finite Fourier transform was applied, whereas in the second stage the double Fourier series and Lardy's method were used to find solution to the plate buckling problem in two cases of boundary conditions of the plate: i.e., freely supported on the whole circumference and clamped along two opposite edges and freely supported on the remaining boundaries. In both considered cases the solution of the problem was reduced to the infinite linear homogeneous algebraic systems of equations.

The results of computations which are of great practical significance are presented in the form of tables and figures which can immediately be used in engineering practice.

1. INTRODUCTION

The subject of this paper is the problem of buckling of an elastic isotropic homogeneous small thickness rectangular plate loaded in an arbitrary way along its boundaries.

Although the problems of elastic stability of the rectangular plate may be considered as classic ones and are widely described in the literature [2, 4, 8, 9, 11, 12], the known solutions however do not include many important cases occuring frequently in engineering structures. It is worth mentioning here the problems of buckling of the plates loaded along boundaries curvilinearly or linearly but in a discontinuous manner, i.e., on certain segments.

From this range of problems we may cite only a few solutions which are mostly approximate solutions. One of them is an approximate solution given by W. NOWACKI [5] concerning the buckling problem of the rectangular plate subjected to the action of the point forces applied to two opposite boundaries. This solution constitutes a generalization of the known Sommerfeld solution and consists of the buckling of the rectangular plate freely supported on the remaining two boundaries.

N. Yamaki applying the Galerkin method evaluated in [13] the critical load for several cases of support of the rectangular plate loaded by two-point forces applied at the centres of the opposite boundaries and for the rectangular plate loaded simply-linearly on certain segments of two opposite edges.

It is much more mathematically difficult to otbain the formal closed solution of the bucling problem for the plate subjected to the action of the curvilinear or linear discontinuous load along boundaries than for the plate loaded along boundaries in a linear continuous way. The reason for this fact lies in a feature of the solution of the shield problem because only in the case of simply-linear and continuous loads along boundaries we obtain identical distributions of the internal forces in the shield. The other loads of the boundary cause in the shield the internal forces distributions different in particular sections and prescribed by means of the function of two variables. Taking into account such functions in the differential equation describing the plate buckling problem complicates its solution significantly.

In this paper a method for the solution of the buckling problem of rectangular plates loaded arbitrarily along the boundaries is presented. The generality of the considerations enables us the use of the proposed method of solution to the computation of the critical parameters in different cases of the curvilinear and discontinuous loads along edges and for different boundary conditions. The problem of buckling of the plate subjected to the action of a uniform load distributed along certain segments of the edges is examined in detail.

The solution presented contains two stages, i.e., the evaluation of the distributions of the internal forces in a shield and computation of the critical load causing the buckling of the plate. Two kinds of boundary conditions are considered, namely the plate freely supported along its circumference and the plate clamped on two opposite boundaries and the free supports on the two remaining boundaries.

The solution of the problem was reduced to the infinite systems of the linear homogeneous algebraic equations. Thanks to the use of the digital computer the critical loads were evaluated for different ratio of the plate dimensions and for different length of the segments of the loaded boundary.

2. Some formulae concerning the finite Fourier transforms used in this paper

The finite sine- cosine transform of the function of two variables in a region $0 \leqslant x \leqslant a$, $0 \leqslant y \leqslant b$ is defined by means of the formula [1]:

$$T_{mn}^{rs}[f(x,y)] = \int_0^a \int_0^b f(x,y)\, \varphi_r(\alpha_m x)\, \varphi_s(\beta_n y)\, dx\, dy, \tag{2.1}$$

where

$$\alpha_m = \frac{m\pi}{a}, \qquad \beta_n = \frac{n\pi}{b}, \qquad r, s = 1, 2, \qquad m, n = 0, 1, 2, \ldots$$

and the symbols φ_1 and φ_2 denote sine and cosine, respectively. The function $f(x, y)$ may be presented in the form of the double Fourier series

$$f(x,y) = \frac{4}{ab} \sum_{m=0,1,2,\ldots}^{\infty} \; \sum_{n=0,1,2,\ldots}^{\infty} \lambda_{mn}\, T_{mn}^{rs}[f(x,y)]\, \varphi_r(\alpha_m x)\, \varphi_s(\beta_n y), \tag{2.2}$$

where

$$\lambda_{mn}=\lambda_m \lambda_n,$$

(2.3)
$$\lambda_m, \lambda_n=\begin{cases}\frac{1}{2} & \text{for } m, n=0,\\ 1 & \text{for } m, n\neq 0.\end{cases}$$

The transforms of the derivatives of the function $f(x, y)$ are obtained by integrating by parts of the expression (2.1)

(2.4)
$$T^{1r}_{mn}\left(\frac{\partial f}{\partial x}\right)=-\alpha_m T^{2r}_{mn}(f), \qquad T^{r1}_{mn}\left(\frac{\partial f}{\partial y}\right)=-\beta_n T^{r2}_{mn}(f),$$
$$T^{2r}_{mn}\left(\frac{\partial f}{\partial x}\right)=B^{1r}_{mn}(f)+\alpha_m T^{1r}_{mn}(f),$$
$$T^{r2}_{mn}\left(\frac{\partial f}{\partial y}\right)=B^{2r}_{mn}(f)+\beta_n T^{r1}_{mn}(f);$$

where

(2.5)
$$B^{1r}_{mn}(f)=(-1)^m T^r_n[f(a, y)]-T^r_n[f(0, y)],$$
$$B^{2r}_{mn}(f)=(-1)^n T^r_m[f(x, b)]-T^r_m(f(x, 0)].$$

In a similar way we can write the transforms for the boundary conditions

(2.6)
$$B^{21}_{mn}\left(\frac{\partial f}{\partial x}\right)=-\alpha_m B^{22}_{mn}(f),$$
$$B^{11}_{mn}\left(\frac{\partial f}{\partial y}\right)=-\beta_n B^{12}_{mn}(f).$$

The transforms of the product of two functions $f(x, y)$ and $q(x, y)$ one of which is expressed in terms of the double Fourier series

$$q(x, y)=\frac{4}{ab}\sum_{i=0,1,2,\ldots}^{\infty}\sum_{j=0,1,\ldots}^{\infty}\lambda_{ij} T^{rs}_{ij}(g)\,\varphi_r(\alpha_i x)\,\varphi_s(\beta_j y),$$

are written in the form

(2.7)
$$T^{klrs}_{mn}(f, q)=\frac{4}{ab}\sum_{i=0,1,\ldots}^{\infty}\sum_{j=0,1,\ldots}^{\infty}\lambda_{ij} T^{rs}_{ij}(q)\, T^{rskl}_{ijmn}(f),$$

where

$$T^{rskl}_{ijmn}(f)=T^{kl}_{mn}[f(x, y)\,\varphi_r(\alpha_i x)\,\varphi_s(\beta_j y)].$$

3. Determination of the state of stress in a shield loaded discontinuously on the boundaries

The plane state of stress in a shield is described by the known system of the differential equations:

(3.1)
$$\frac{\partial N_1}{\partial x}+\frac{\partial N_{12}}{\partial y}=0, \qquad \frac{\partial N_{12}}{\partial x}+\frac{\partial N_2}{\partial y}=0,$$

where

$$N_1=A\left(\frac{\partial u}{\partial x}+\nu\frac{\partial u}{\partial x}\right),\quad N_2=A\left(\frac{\partial v}{\partial y}+\nu\frac{\partial u}{\partial x}\right),\quad N_{12}=B\left(\frac{\partial u}{\partial y}+\frac{\partial v}{\partial x}\right),\tag{3.2}$$

and

$$A=\frac{Eh}{(1-\nu^2)},\quad B=\frac{Eh}{2(1+\nu)}.\tag{3.3}$$

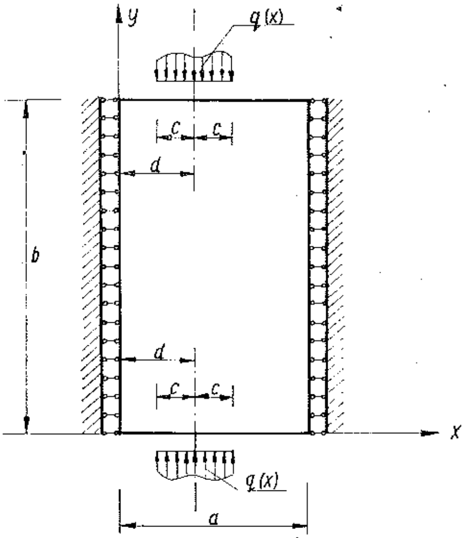

Fig. 1

In expressions (3.1) and (3.2), $N_1=N_1(x,y)$, $N_2=N_2(x,y)$, $N_{12}=N_{12}\times(x,y)$ denote internal forces, $u=u(x,y)$, $v=v(x,y)$ are the displacements of the points, of the shield plane in directions of the axes x and y (Fig. 1), E, h, and ν are the Young modulus, shield thickness and Poisson number, respectively.

Performing the Fourier transform according to the formula (2.1) to the system of the Eqs. (3.1) we obtain

$$\begin{aligned}&T^{12}_{mn}\left(\frac{\partial N_1}{\partial x}+\frac{\partial N_{12}}{\partial y}\right)=0,\\&T^{21}_{mn}\left(\frac{\partial N_{12}}{\partial x}+\frac{\partial N_2}{\partial y}\right)=0.\end{aligned}\tag{3.4}$$

Using formulae (2.4) and (2.6) the system of the Eqs. (3.4) may be written in the form

$$\begin{aligned}&-\alpha_m T^{22}_{mn}(N_1)+\beta_n T^{11}_{mn}(N_{12})+B^{21}_{mn}(N_{12})=0,\\&\alpha_m T^{11}_{mn}(N_{12})-\beta_n T^{22}_{mn}(N_2)+B^{11}_{mn}(N_{12})=0.\end{aligned}\tag{3.5}$$

Applying the Fourier transform (2.1) to the expressions (3.2) we find

$$\begin{aligned}&T^{22}_{mn}(N_1)=A\left[\alpha_m u_{mn}+U^{(1)}_{mn}+\nu(\beta_n v_{mn}+V^{(1)}_{mn})\right],\\&T^{22}_{mn}(N_2)=A\left[\beta_n v_{mn}+V^{(1)}_{mn}+\nu(\alpha_m u_{mn}+U^{(1)}_{mn})\right],\\&T^{11}_{mn}(N_{12})=-B(\alpha_m v_{mn}+\beta_n u_{mn}),\end{aligned}\tag{3.6}$$

where

$$\begin{aligned}&u_{mn}=T^{12}_{mn}(u),\quad U^{(1)}_{mn}=B^{12}_{mn}(u),\\&v_{mn}=T^{21}_{mn}(v),\quad V^{(1)}_{mn}=B^{21}_{mn}(v).\end{aligned}\tag{3.7}$$

After substitution of the expressions (3.6) to the system of the Eqs. (3.5) we obtain

$$\begin{aligned}&(A\alpha_m^2+B\beta_n^2)u_{mn}+(A\nu+B)\alpha_m\beta_n v_{mn}+A\alpha_m(U^{(1)}_{mn}+\nu V^{(1)}_{mn})-N^{(2)}_{mn}=0,\\&(A\nu+B)\alpha_m\beta_n u_{mn}+(A\beta_n^2+B\alpha_m^2)v_{mn}+B\beta_n(V^{(1)}_{mn}+\nu U^{(1)}_{mn})-N^{(1)}_{mn}=0,\end{aligned}\tag{3.8}$$

where

$$N_{mn}^{(1)}=B_{mn}^{11}(N_{12}), \qquad N_{mn}^{(2)}=B_{mn}^{21}(N_{12}). \tag{3.9}$$

Solving the system of the Eqs. (3.8) with respect to the unknown u_{mn} and v_{mn} we get

$$\begin{aligned} u_{mn}&=\frac{1}{\Delta_{mn}}\Big\{\alpha_m(\beta_n^2-\nu\alpha_m^2)V_{mn}^{(1)}-\alpha_m[\alpha_m^2+(2+\nu)\beta_n^2]U_{mn}^{(1)}+\\ &\qquad+\frac{1}{AB}[(A\beta_n^2+B\alpha_m^2)N_{mn}^{(2)}-(A\nu+B)\alpha_m\beta_n N_{mn}^{(1)}]\Big\},\\ v_{mn}&=\frac{1}{\Delta_{mn}}\Big\{\beta_n(\alpha_m^2-\nu\beta_n^2)U_{mn}^{(1)}-\beta_n[\beta_n^2+(2+\nu)\alpha_m^2]V_{mn}^{(1)}+\\ &\qquad+\frac{1}{AB}[(A\alpha_m^2+B\beta_n^2)N_{mn}^{(1)}-(A\nu+B)\alpha_m\beta_n N_{mn}^{(2)}]\Big\}, \end{aligned} \tag{3.10}$$

where

$$\Delta_{mn}=(\alpha_m^2+\beta_n^2)^2. \tag{3.11}$$

Consider the shield supported and loaded as it is shown in Fig. 1. Then the following boundary conditions hold:

$$\begin{aligned} &u(0,y)=u(a,y)=0,\\ &N_2(x,0)=N_2(x,b)=-q(x),\\ &N_{12}(0,y)=N_{12}(a,y)=N_{12}(x,0)=N_{12}(x,b)=0. \end{aligned} \tag{3.12}$$

Using boundary conditions (3.12) and the expressions (2.5) (3.7) and (3.9) we obtain

$$\begin{aligned} &U_{mn}^{(1)}=N_{mn}^{(1)}=N_{mn}^{(2)}=0,\\ &V_{mn}^{(1)}=(-1)^m T_m^2[v(x,b)]-T_m^2[v(x,0)]. \end{aligned} \tag{3.13}$$

After substitution of the expressions (3.13) into the formula (3.10) we have

$$\begin{aligned} u_{mn}&=\frac{\alpha_m}{\Delta_{mn}}(\beta_n^2-\nu\alpha_m^2)V_{mn}^{(1)},\\ v_{mn}&=-\frac{\beta_n}{\Delta_{mn}}[\beta_n^2+(2+\nu)\alpha_m^2]V_{mn}^{(1)}. \end{aligned} \tag{3.14}$$

The functions describing the displacement of the points of the shield edges appearing in the Eq. (3.13) and the load function $q(x)$ may be expressed in terms of the single Fourier series:

$$\begin{aligned} v(x,0)&=-v(x,b)=\frac{2}{a}\sum_{m=0,1,2,\dots}^{\infty}\lambda_m v_m^{(1)}\cos\alpha_m x,\\ q(x)&=\frac{2}{a}\sum_{m=0,1,2,\dots}^{\infty}\lambda_m q_m\cos\alpha_m x. \end{aligned} \tag{3.15}$$

Substituting the Eq. (3.15) into the Eq, (3.13) and using formulae (3.14), (3.6), and (2.2) we obtain the double Fourier series describing the distributions of the internal forces in a region of the shield

$$
\begin{aligned}
N_1(x,y) &= -\frac{2\nu A}{ab}\, v_0^{(1)} - \\
&\quad -\frac{8A}{ab}(1-\nu^2) \sum_{m=1,2,3,\dots}^{\infty} \; \sum_{n=2,4,6,\dots}^{\infty} \frac{v_m^{(1)}}{\Delta_{mn}}\, \alpha_m^2 \beta_n^2 \cos\alpha_m x \cos\beta_n y, \\
N_2(x,y) &= -\frac{2A}{ab}\, v_0^{(1)} - \\
&\quad -\frac{4A}{ab}(1-\nu^2) \sum_{m=1,2,3,\dots}^{\infty} v_m^{(1)} \left[1 + 2\alpha_m^4 \sum_{n=2,4,6,\dots}^{\infty} \frac{1}{\Delta_{mn}} \cos\beta_n y\right] \cos\alpha_m x, \\
N_2(x,y) &= -\frac{16B}{ab}(1-v^2) \sum_{m=1,2,3,\dots}^{\infty} \; \sum_{n=2,4,6,\dots}^{\infty} \frac{v_m^{(1)}}{\Delta_{mn}}\, \alpha_m^3 \beta_n \sin\alpha_m x \sin\beta_n y.
\end{aligned}
\tag{3.16}
$$

After substitution of the series (3.16) and (3.15) to the boundary conditions (3.12) we have:

$$
\begin{aligned}
v_0^{(1)} &= \frac{b}{2A} q_0, \\
v_m^{(1)} &= \frac{b q_m}{2A(1-\nu^2)\left[1 + 2\alpha_m^4 \sum\limits_{n=2,4,6,\dots}^{\infty} \frac{1}{\Delta_{mn}}\right]}.
\end{aligned}
\tag{3.17}
$$

The sums of the series appearing in the formulae (3.16) and (3.17) are as follows:

$$
\begin{aligned}
&\sum_{n=2,4,6,\dots}^{\infty} \frac{\beta_n}{\Delta_{mn}} \sin\beta_n y = \frac{b}{8\alpha_m^2 \operatorname{sh}^2\kappa_m}\left[\alpha_m y \operatorname{sh}\kappa_m \operatorname{ch}\alpha_m\left(y-\frac{b}{2}\right) - \kappa_m \operatorname{sh}\alpha_m y\right], \\
&\sum_{n=2,4,6,\dots}^{\infty} \frac{\beta_n^2}{\Delta_{mn}} \cos\beta_n y = \frac{b}{8\alpha_m \operatorname{sh}^2\kappa_m}\left[\operatorname{sh}\kappa_m \operatorname{ch}\alpha_m\left(y-\frac{b}{2}\right) + \right. \\
&\qquad\qquad \left. + \alpha_m y \operatorname{sh}\kappa_m \operatorname{sh}\alpha_m\left(y-\frac{b}{2}\right) - \kappa_m \operatorname{ch}\alpha_m y\right], \\
&1 + 2\alpha_m^4 \sum_{n=2,4,6,\dots}^{\infty} \frac{1}{\Delta_{mn}} \cos\beta_n y = \frac{\kappa_m}{2\operatorname{sh}^2\kappa_m}\left[\operatorname{sh}\kappa_m \operatorname{ch}\alpha_m\left(y-\frac{b}{2}\right) - \right. \\
&\qquad\qquad \left. - \alpha_m y \operatorname{sh}\kappa_m \operatorname{sh}\alpha_m\left(y-\frac{b}{2}\right) + \kappa_m \operatorname{ch}\alpha_m y\right], \\
&1 + 2\alpha_m^4 \sum_{n=2,4,6,\dots}^{\infty} \frac{1}{\Delta_{mn}} = \frac{\kappa_m}{4\operatorname{sh}^2\kappa_m}(2\kappa_m + \operatorname{sh} 2\kappa_m),
\end{aligned}
\tag{3.18}
$$

where $\kappa_m = \alpha_m b/2$.

Substituting the determined sums of series (3.18) into the formula (3.16) and using relations (3.17) we obtain the single Fourier series describing the distributions of the internal forces in the shield

$$\begin{aligned} N_1(x,y) &= -\nu\frac{q_0}{a} - \frac{4}{a}\sum_{m=1,2,3,\ldots}^{\infty}\frac{q_m}{(2\kappa_m+\operatorname{sh}2\kappa_m)}\left[\operatorname{sh}\kappa_m\operatorname{ch}\alpha_m\left(y-\frac{b}{2}\right)+\right.\\ &\qquad\left.+\alpha_m y\operatorname{sh}\kappa_m\operatorname{sh}\alpha_m\left(y-\frac{b}{2}\right)-\kappa_m\operatorname{ch}\alpha_m y\right]\cos\alpha_m x,\\ N_2(x,y) &= -\frac{q_0}{a} - \frac{4}{a}\sum_{m=1,2,3,\ldots}^{\infty}\frac{q_m}{(2\kappa_m+\operatorname{sh}2\kappa_m)}\left[\operatorname{sh}\kappa_m\operatorname{ch}\alpha_m\left(y-\frac{b}{2}\right)-\right.\\ &\qquad\left.-\alpha_m y\operatorname{sh}\kappa_m\operatorname{sh}\alpha_m\left(y-\frac{b}{2}\right)+\kappa_m\operatorname{ch}\alpha_m y\right]\cos\alpha_m x,\\ N_{12}(x,y) &= -\frac{4}{a}\sum_{m=1,2,3,\ldots}^{\infty}\frac{q_m}{(2\kappa_m+\operatorname{sh}2\kappa_m)}\times\\ &\qquad\times\left[\alpha_m y\operatorname{sh}\kappa_m\operatorname{ch}\alpha_m\left(y-\frac{b}{2}\right)-\kappa_m\operatorname{sh}\alpha_m y\right]\sin\alpha_m x. \end{aligned} \tag{3.19}$$

Identical series were obtained while solving the problem considered by means of a single Fourier series and with use of the displacements functions.

The distributions of the interior forces in the shield we shall determine for a case of the load uniformly distributed on the segment of the shield boundary of the length equal to $2c$ (Fig. 1), $q(x)=q=\text{const}$ and $d/a=0.5$.

Thus on the basis of formula (2.1) we find:

$$\begin{aligned} q_0 &= 2qc,\\ q_m &= 2(-1)^{\frac{m}{2}}\frac{q}{\alpha_m}\sin\alpha_m c, \qquad m=2,4,6,\ldots. \end{aligned} \tag{3.20}$$

We assume further the following dimensionless coordinates

$$\xi=\frac{x}{a},\qquad \eta=\frac{y}{b},\qquad \varepsilon=\frac{c}{a},\qquad \mu=\frac{b}{a},$$

and the value of the Poisson number $\nu=0.25$.

The numerical values of the internal forces computed on the digital computer ODRA 1204 in different points of the shield for the chosen values of ε and μ are presented in Tables 1 and 2, on the basis of which the corresponding diagrams are made. For $\varepsilon=0.25$, $\mu=1.00$ the verification of the results computed was performed by means of the finite difference method and a practically good agreement was achieved. In Fig. 3 the broken line denotes the ordinates computed by use of the finite difference method.

Table 1

ξ	$\varepsilon = \frac{1}{4}$, $\mu = 0.5$: $\frac{1}{q} N_1$	$\frac{1}{q} N_2$	$\frac{1}{q} N_{12}$	$\varepsilon = \frac{1}{4}$, $\mu = 1.0$: $\frac{1}{q} N_1$	$\frac{1}{q} N_2$	$\frac{1}{q} N_{12}$
			$\eta = 0.00$			
0.0	0.56372	—	—	0.34058	—	—
0.10	0.69273	—	—	0.38230	—	—
0.20	0.77278	—	—	0.36171	—	—
0.30	-1.02280	1.00000	—	-0.61171	1.00000	—
0.40	-0.94273	1.00000	—	-0.63230	1.00000	—
0.50	-0.81372	1.00000	—	-0.59058	1.00000	—
			$\eta = 0.10$			
0.0	0.31972	0.31678	—	0.01124	-0.02627	—
0.10	0.27300	0.34286	-0.03035	-0.02866	-0.04729	0.06347
0.20	-0.01783	0.26993	0.18618	-0.12696	-0.22668	0.22273
0.30	-0.23217	-1.26990	0.18618	-0.12304	-0.77332	0.22273
0.40	-0.52300	-1.34290	-0.05035	-0.22134	-0.95271	0.06347
0.50	-0.56972	-1.31680	—	-0.26124	-0.97373	—
			$\eta = 0.20$			
0.0	0.05001	0.39427	—	-0.17243	-0.10033	—
0.10	-0.01451	0.36146	0.00438	-0.17625	-0.15370	0.10214
0.20	-0.16080	+ 0.03096	0.24056	-0.15568	-0.35094	0.20448
0.30	-0.08920	-1.03100	0.24056	-0.09432	-0.64096	0.20448
0.40	-0.23549	-1.36150	0.00438	-0.07375	-0.84630	0.10214
0.50	-0.30001	-1.39430	—	-0.07757	-0.89967	—
			$\eta = 0.30$			
0.0	-0.15147	0.44150	—	-0.22989	-0.19278	—
0.10	-0.18717	0.35012	0.02948	-0.21373	-0.24592	0.08131
0.20	-0.19538	-0.08783	0.18714	-0.16128	-0.39953	0.14049
0.30	-0.05462	-0.91217	0.18714	-0.08871	-0.60047	0.14049
0.40	-0.06283	-1.35010	0.02948	-0.03627	-0.75408	0.08131
0.50	-0.09853	-1.44150	—	-0.02011	-0.80722	—
			$\eta = 0.40$			
0.0	-0.27466	0.46568	—	-0.23956	-0.25646	—
0.10	-0.27918	0.34140	0.02409	-0.21854	-0.30216	0.04204
0.20	-0.21107	-0.13960	0.09911	-0.16126	-0.42363	0.06978
0.30	-0.03893	-0.86040	0.09911	-0.08874	-0.57637	0.06978
0.40	0.02918	-1.34140	0.02409	-0.03146	-0.69784	0.04204
0.50	0.02466	-1.46570	—	-0.01043	-0.74354	—
			$\eta = 0.50$			
0.0	-0.32579	0.48204	—	-0.23963	-0.27812	—
0.10	-0.31659	0.34311	—	-0.21797	-0.32021	—
0.20	-0.21958	-0.14791	—	-0.16074	-0.43104	—
0.30	-0.03042	-0.85209	—	-0.08925	-0.56896	—
0.40	0.06659	-1.34310	—	-0.03203	-0.67979	—
0.50	0.07579	-1.48200	—	-0.01037	-0.72188	—

Table 2

ξ	ε = 1/60, μ = 0.5: $\frac{1}{q}N_1$	$\frac{1}{q}N_2$	$\frac{1}{q}N_{12}$	ε = 1/60, μ = 2.0: $\frac{1}{q}N_1$	$\frac{1}{q}N_2$	$\frac{1}{q}N_{12}$
			η = 0.00			
0.0	0.07374	———	———	0.01859	———	———
0.10	-0.00458	———	———	-0.00188	———	———
0.20	0.08752	———	———	0.01840	———	———
0.30	0.02618	———	———	-0.00125	———	———
0.40	0.10962	———	———	0.01518	———	———
0.50	-0.01697	1.00000	———	-0.43848	1.00000	———
			η = 0.10			
0.0	0.02057	0.01736	———	-0.00818	-0.01873	———
0.10	0.02314	0.01666	-0.00563	-0.00885	-0.01937	0.00271
0.20	0.01957	0.02809	-0.00749	-0.01667	-0.02206	0.00660
0.30	0.00815	0.03431	-0.00612	-0.01198	-0.03023	0.01271
0.40	-0.07002	0.01156	0.06242	-0.00685	-0.05085	0.01661
0.50	0.03648	-0.72930	———	0.00158	-0.06965	———
			η = 0.20			
0.0	0.00902	0.02355	———	-0.011658	-0.02502	———
0.10	0.00665	0.02543	-0.00634	-0.01135	-0.02610	0.00305
0.20	-0.00210	0.02859	-0.00878	-0.01021	-0.02947	0.00572
0.30	-0.02327	0.02041	0.00724	-0.00786	-0.03509	0.00698
0.40	-0.05013	-0.07028	0.08584	-0.00480	-0.04135	0.00514
0.50	0.05625	-0.38017	———	0.00324	-0.04429	———
			η = 0.30			
0.0	-0.00253	0.03040	———	-0.01039	-0.02977	———
0.10	-0.00631	0.03105	-0.00514	-0.01005	-0.03038	0.00155
0.20	-0.01711	0.02793	-0.00544	-0.00909	-0.03207	0.00253
0.30	-0.03008	0.000407	0.01311	-0.00776	-0.03435	0.00278
0.40	-0.01293	-0.11030	0.06147	-0.00655	-0.03638	0.00180
0.50	0.05284	-0.26284	———	-0.00605	-0.03720	———
			η = 0.40			
0.0	-0.01089	0.035417	———	-0.00931	-0.03188	———
0.10	-0.01508	0.03488	-0.00276	-0.00913	-0.03215	0.00055
0.20	-0.02501	0.02637	-0.00224	-0.00865	-0.03287	0.00091
0.30	-0.02785	-0.01458	0.00929	-0.00804	-0.03377	0.00092
0.40	0.00828	-0.12283	0.02980	-0.00752	-0.03452	0.00058
0.50	0.05093	-0.21648	———	-0.00732	-0.03482	———
			η = 0.50			
0.0	-0.01496	0.03828	———	-0.00899	-0.03243	———
0.10	-0.01902	0.03709	———	-0.00886	-0.03260	———
0.20	-0.02776	0.02599	———	-0.00854	-0.03305	———
0.30	-0.02589	-0.02019	———	-0.00813	-0.03361	———
0.40	0.01272	-0.12628	———	-0.00780	-0.03407	———
0.50	0.05155	-0.20485	———	-0.00767	-0.03424	———

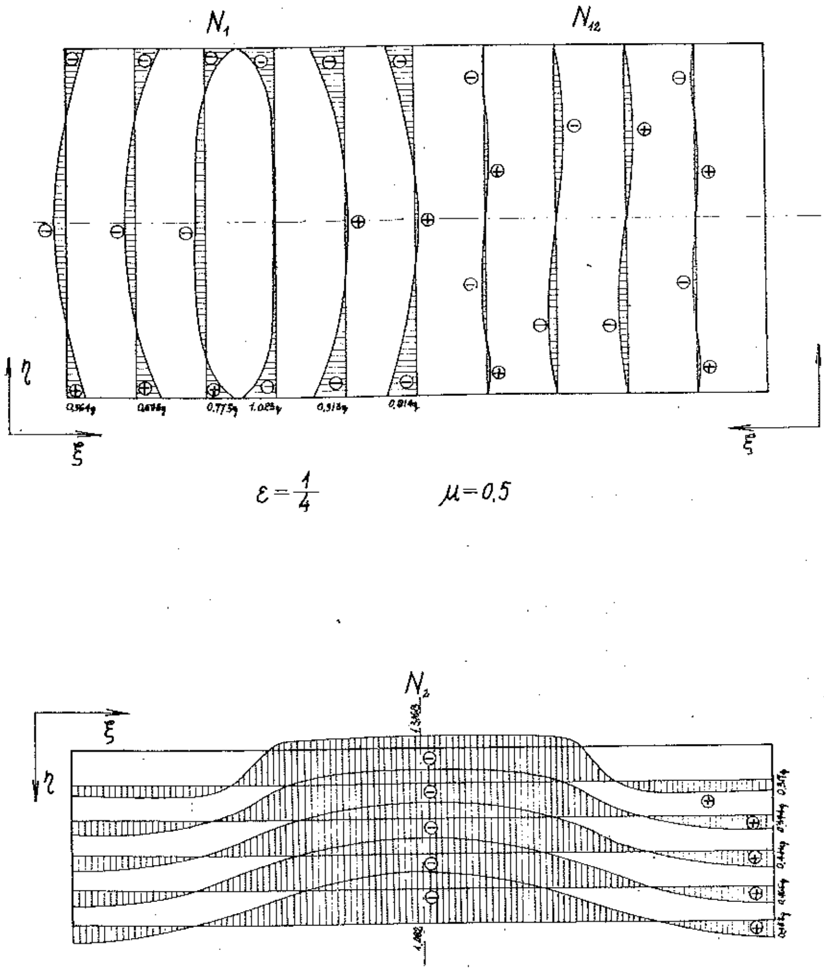

Fig. 2

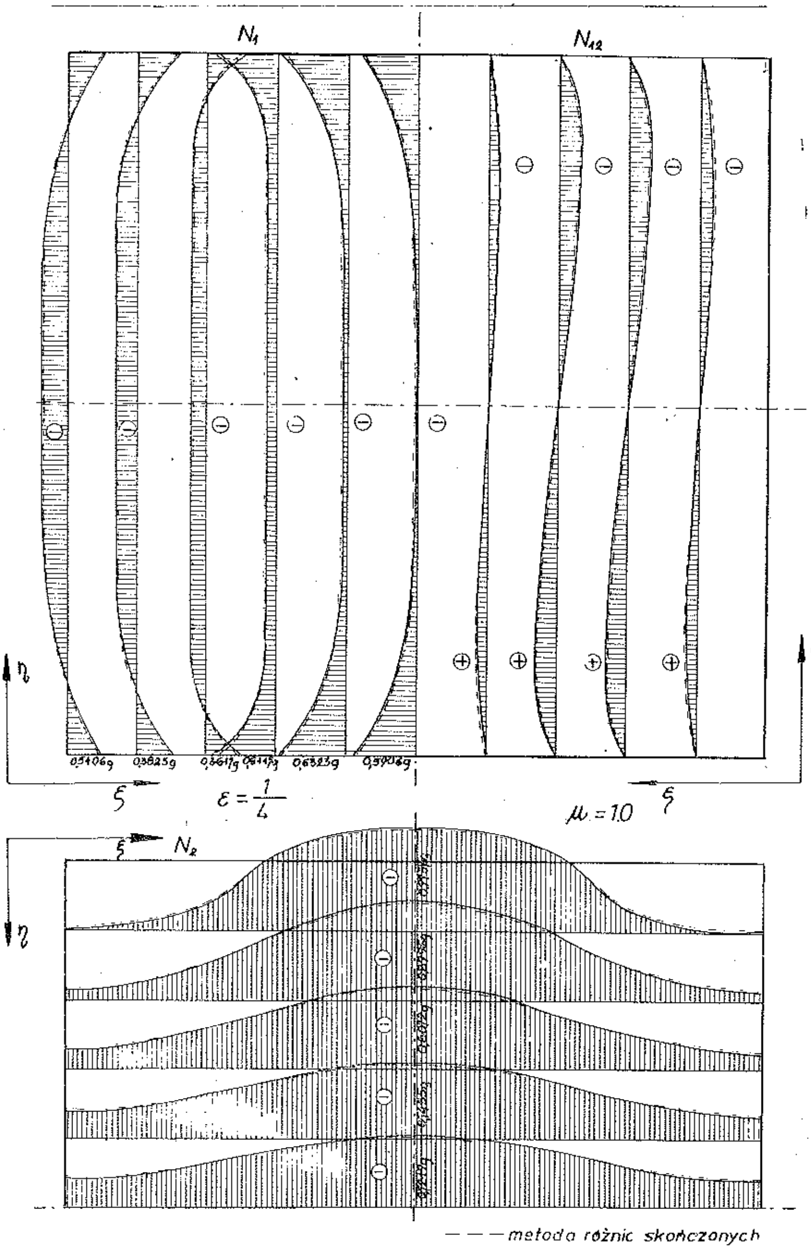

N1
N12
0,5406g
0,3825g
0,3617g
0,6323g
0,5906g
ε = 1/4
μ = 1,0
N2
— — — metoda różnic skończonych

Fig. 3

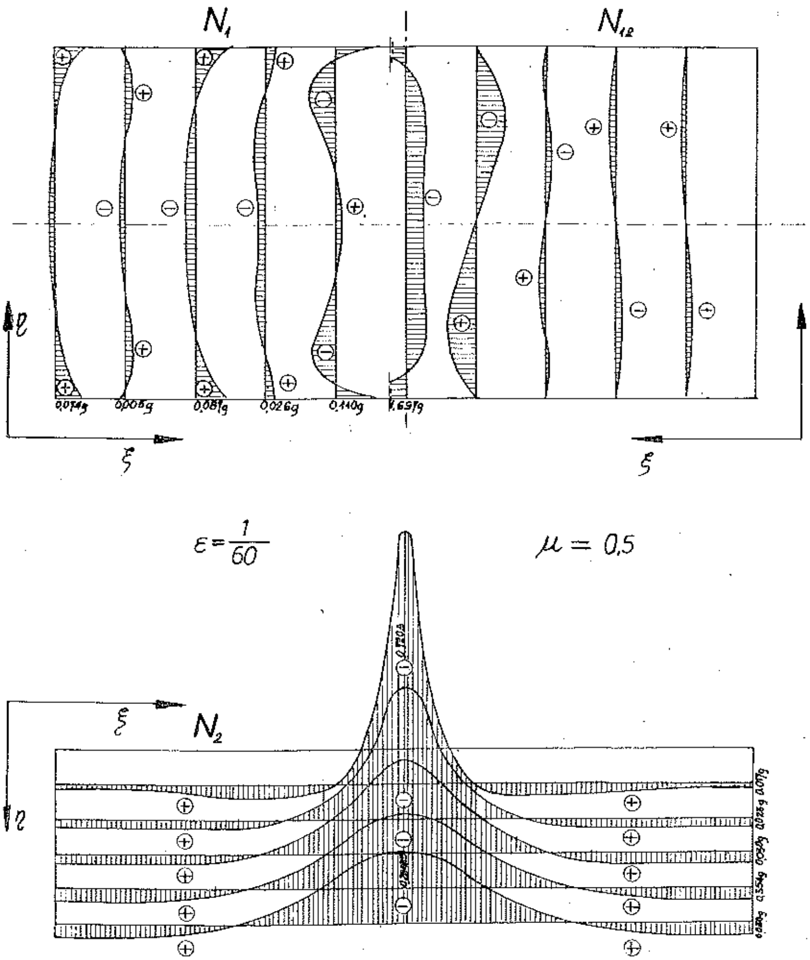
N_1
N_{12}
0,074g
0,008g
0,081g
0,026g
0,110g
1,691g
ξ
η
$\varepsilon = \frac{1}{60}$
$\mu = 0{,}5$
N_2

Fig. 4

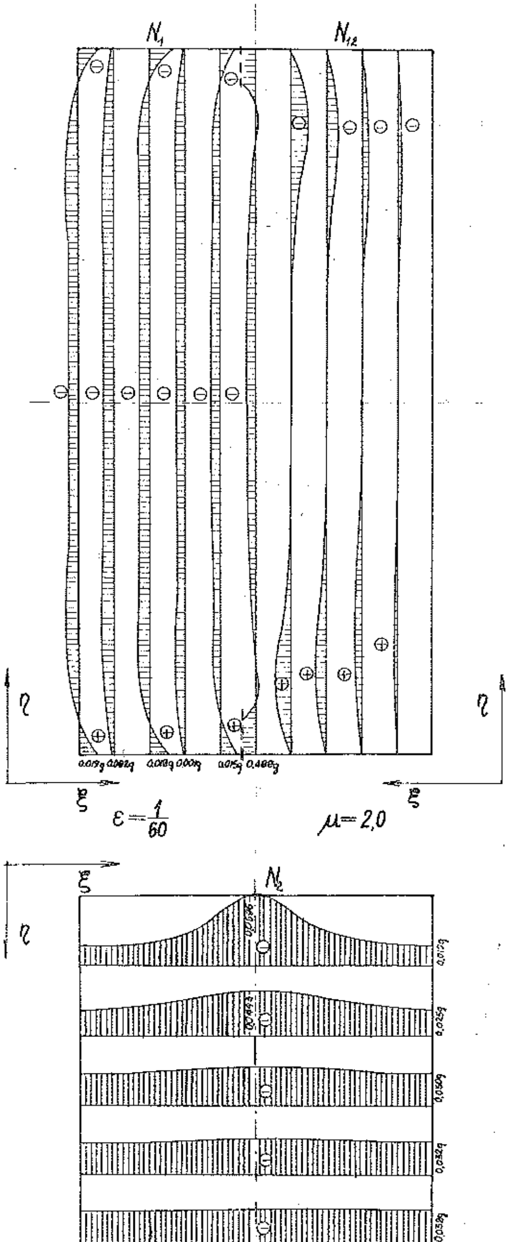

Fig. 5

4. Buckling of the plate freely supported on the circumference

The subject of the considerations of this section is a problem of the elastic buckling of the isotropic plate freely supported along the whole circumference and subjected along boundaries $y=0$, $y=b$ to the action of the discontinuous load $p(y)$ which does not permit for the horizontal displacement of these edges (Fig. 6).

The solution of the problem is reduced to the evaluation of the eigenvalues of the equations

$$D\nabla^4 w = N_1 \frac{\partial^2 w}{\partial x^2} + 2N_{12}\frac{\partial^2 w}{\partial xy} + N_2 \frac{\partial^2 w}{\partial y^2}, \tag{4.1}$$

where $w=w(x, y)$ is deflection of the plate, $D=\dfrac{Eh^3}{12(1-\nu^2)}$ denotes the bending rigidity of the plate, $N_1=N_1(x, y)$, $N_2=N_2(x, y)$, $N_{12}=N_{12}(x, y)$ are the internal forces acting in the middle surface of the plate which are found from the solution of the shield problem.

The equation of the deflection of the plate subjected to the action of the critical load is expressed in terms of a double Fourier series

$$w(x, y) = \sum_{i=1,2,3,\ldots}^{\infty} \sum_{j=1,2,3,\ldots}^{\infty} w_{ij} \sin\alpha_i x \sin\beta_j y. \tag{4.2}$$

Substituting Eq. (4.2) into the Eq. (4.1) and orthogonalizing this equation with respect to the function $\sin\alpha_k x \sin\beta_l y$ the following infinite system of the linear homogeneous algebraic equations is obtained:

$$\sum_{i=1,2,3,\ldots}^{\infty} \sum_{j=1,2,3,\ldots}^{\infty} w_{ij} A_{klij}=0, \qquad k, l=1,2,3,\ldots, \tag{4.3}$$

where

$$A_{klij} = \frac{ab}{4} D\Delta_{ij}\delta_{ik}\delta_{jl} + E_{klij} \tag{4.4}$$

and

$$\begin{aligned}
E_{klij} &= \alpha_i^2 r_{klij} - 2\alpha_i\beta_j s_{klij} + \beta_i^2 t_{klij},\\
r_{klij} &= \int_0^a\int_0^b N_1(x, y)\sin\alpha_i x \sin\beta_j y \sin\alpha_k x \sin\beta_l y\, dx\, dy,\\
s_{klij} &= \int_0^a\int_0^b N_{12}(x, y)\cos\alpha_i x \cos\beta_j y \sin\alpha_k x \sin\beta_l y\, dx\, dy,\\
t_{klij} &= \int_0^a\int_0^b N_2(x, y)\sin\alpha_i x \sin\beta_j y \sin\alpha_k x \sin\beta_l y\, dx\, dy,
\end{aligned} \tag{4.5}$$

δ_{ik} and δ_{jl} denote the Kronecker's symbols.

By equating to zero the determinant of the basic system of the Eqs. (4.4) we obtain the characteristic equation

$$\det |A_{klij}| = 0, \tag{4.6}$$

the smallest root of which enables us to determine the critical load.

Substituting the series (3.19) into the formula (4.5) and performing integrating and the simple transformations, the integrals (4.6) are reduced to the following form for $i \neq k$, $j \neq i$

$$\begin{aligned} r_{klij} &= bq_{i+k}\kappa_{i+k}S_{i+k}\left(\frac{\gamma_{j-l}^2}{\Delta_{i+k,\,j-l}} - \frac{\gamma_{j+l}^2}{\Delta_{i+k,\,j+l}}\right) + \\ &\qquad + bq_{i-k}\kappa_{i-k}S_{i-k}\left(\frac{\gamma_{j+l}^2}{\Delta_{i-k,\,j+l}} - \frac{\gamma_{j-l}^2}{\Delta_{i-k,\,j-l}}\right), \\ s_{klij} &= bq_{i+k}\kappa_{i+k}^2 S_{i+k}\left(\frac{\gamma_{j-l}}{\Delta_{i+k,\,j-l}} - \frac{\gamma_{j+l}}{\Delta_{i+k,\,j+l}}\right) + \\ &\qquad + bq_{i-k}\kappa_{i-k}^2 S_{i-k}\left(\frac{\gamma_{j+l}}{\Delta_{i-k,\,j+l}} - \frac{\gamma_{j-l}}{\Delta_{i-k,\,j-l}}\right), \\ t_{klij} &= bq_{i+k}\kappa_{i+k}^3 S_{i+k}\left(\frac{1}{\Delta_{i+k,\,j-l}} - \frac{1}{\Delta_{i+k,\,j+l}}\right) + \\ &\qquad + bq_{i-k}\kappa_{i-k}^3 S_{i-k}\left(\frac{1}{\Delta_{i-k,\,j+l}} - \frac{1}{\Delta_{i-k,\,j-l}}\right), \end{aligned} \tag{4.7}$$

where

$$\begin{aligned} &\kappa_{i\pm k} = \kappa_i \pm \kappa_k, \quad \kappa_r = \alpha_r \frac{b}{2}, \quad r = i, k, \quad j+l = 2, 4, 6, \ldots, \\ &\gamma_{j\pm l} = \gamma_j \pm \gamma_l, \quad \gamma_u = \beta_u \frac{b}{2}, \quad u = j, l, \quad i \pm k = 1, 3, 5, \ldots, \\ &S_{i\pm k} = \frac{\operatorname{sh}^2 \kappa_{i\pm k}}{2\kappa_{i\pm k} + \operatorname{sh} 2\kappa_{i\pm k}}, \quad \Delta_{i\pm k,\,j\pm l} = (\kappa_{i+k}^2 + \gamma_{j\pm 1}^2)^2. \end{aligned} \tag{4.8}$$

For $i = k$, $j = l$ we have

$$\begin{aligned} r_{klkl} &= -\nu \frac{b}{4} q_0 - \frac{1}{2\Delta_{kl}} q_{2k}\gamma_l^2 \kappa_k S_{2k}, \\ s_{klkl} &= -\frac{b}{2\Delta_{kl}} q_{2k}\gamma_l \kappa_k^2 S_{2k}, \\ t_{klkl} &= -\frac{b}{4} q_0 + \frac{b}{2\kappa_k \Delta_{kl}} q_{2k}\gamma_l^2 (2\kappa^2 + \gamma_l^2) S_{2k}, \end{aligned} \tag{4.9}$$

where

$$\Delta_{kl} = (\kappa_k^2 + \gamma_l^2)^2, \quad S_{2k} = \frac{\operatorname{sh}^2 2\kappa_k}{4\kappa_k + \operatorname{sh} 4\kappa_k}. \tag{4.10}$$

After substitution of the expressions (4.7) and (4.9) into the Eq. (4.4) we obtain for $i \neq k$ and $j \neq l$

$$(4.11)\quad A_{klij}=\frac{4}{b} q_{i+k}\kappa_{i+k} S_{l+k}\left[\frac{(\gamma_l\kappa_i+\gamma_j\kappa_k)^2}{\Delta_{i+k,\,j-l}}-\frac{(\gamma_l\kappa_i-\gamma_j\kappa_k)^2}{\Delta_{i+k,\,j+l}}\right]+ +\frac{4}{b} q_{i-k}\kappa_{i-k} S_{i-k}\left[\frac{(\gamma_l\kappa_i+\gamma_j\kappa_k)^2}{\Delta_{i-k,\,j+l}}-\frac{(\gamma_l\kappa_i-\gamma_j\kappa_k)^2}{\Delta_{i-k,\,j-l}}\right],$$

$$j\pm l=2,4,6,\ldots,\quad j,l=1,2,3,\ldots,$$

$$i\pm k=1,2,3,\ldots,\quad i,k=1,2,3,\ldots,$$

and for $i=k$, $j=l$

$$(4.12)\quad A_{klkl}=\frac{4}{b^3} Da\,\Delta_{kl}-\frac{1}{a} q_0(\gamma_l^2+\nu\kappa_k^2)+\frac{2}{b\kappa_k} q_{2k}\gamma_l^2 S_{2k},\qquad k,l,=1,2,3,\ldots.$$

The infinite system of the Eqs. (4.3) consists of two independent systems. In the first system the indices run the values $i, k=1, 2, 3, \ldots, j, l=1, 3, 5, \ldots$, in the second system — the values $i, k=1, 2, 3, \ldots, j, l=2, 4, 6, \ldots$.

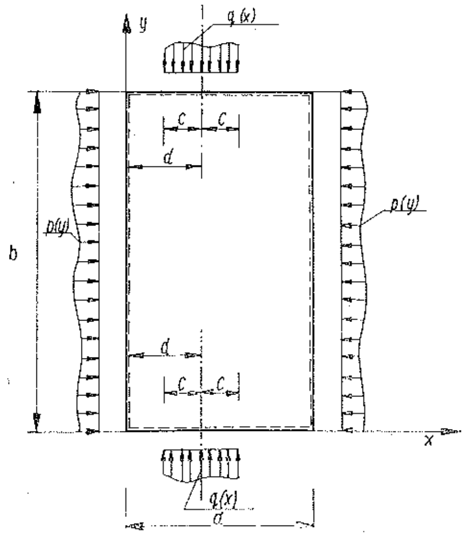

Fig. 6

The critical load corresponding to the smallest value of the root of the characteristic equation (4.6) for indices $i, k=1, 2, 3, \ldots, j, l=1, 3, 5, \ldots$, causes the symmetric mode of the plate buckling in y direction, whereas for the indices $i, k=1, 2, 3, \ldots$, $j, l=2, 4, 6, \ldots$, — the antysymmetric mode.

Table 3 shows the numerical values of the coefficients computed from the Eq. (4.6) with the use of the expressions (4.11), (4.12) and (3.20) for the successive values of ε and μ and for $\nu=0.25$ ([14, 15]). The critical load is evaluated from the formula:

$$(4.13)\qquad P_{cr}=2cq_{cr}=\kappa\frac{D}{a}.$$

Table 3. Values of coefficients 10 κ

ε \ μ	0.5	0.7	1.0	1.25	1.5	1.75	2.0	2.25	2.5	2.75	3.0	3.25	3.5	3.75	4.0
1/4	369	262	239	240	250	260	268	263	261	262	264	267	268	267	267
1/8	310	232	222	222	233	245	250	246	246	247	249	251	252	252	253
1/12	299	226	213	218	230	241	246	243	242	244	245	247	249	249	250
1/16	294	224	211	217	228	240	245	242	242	241	244	246	248	248	249
1/20	292	223	211	216	228	239	244	241	241	242	243	246	247	248	248
1/24	291	223	210	216	227	239	244	241	249	242	243	245	247	247	248

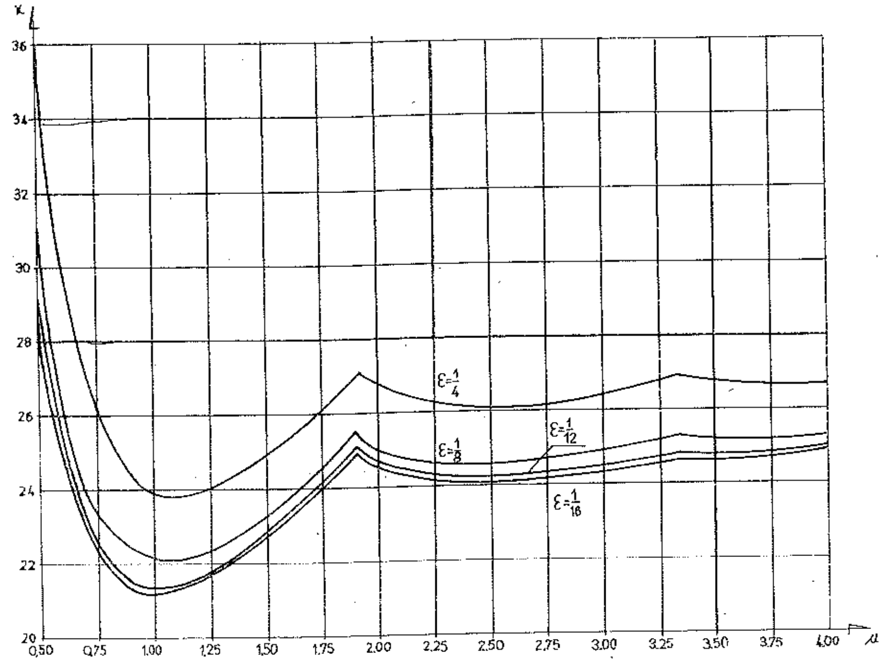

Fig. 7

The corresponding diagrams are shown in Fig. 5. In the case of $\varepsilon=1/4$, $\mu=1.00$ the value of the critical load was verified by means of the finite difference method and practically a good agreement of the results was achieved.

5. Buckling of a plate clamped along the boundaries $x=0$, $x=a$ and freely supported along the boundaries $y=0$, $y=b$

In this case (Fig. 8) an attempt at obtaining the solution by means of the finite Fourier transform has led to very complicated transformations and cumbersome formulae. Therefore this approach was neglected and instead of it the P. Lardy method ([6, 4], p. 402) was used.

The equation for the middle surface of the deformed plate is assumed in the form:

$$w(x,y)=\sum_{i=1,2,3,\ldots}^{\infty}\ \sum_{j=1,2,3,\ldots}^{\infty} w_{ij}\,\varphi_i(x)\,\psi_j(y), \tag{5.1}$$

where $\varphi_i(x)$, $\psi_j(y)$ are the orthogonal functions describing the modes of the eigenvibrations of the rod and satisfying the differential equations

$$\frac{d^4\varphi_i(x)}{dx^4}=\vartheta_i^4\,\varphi_i(x), \qquad \frac{d^4\psi_j(y)}{dy^4}=\beta_j^4\,\psi_j(y), \tag{5.2}$$

with the following boundary conditions

$$\varphi_i(0)=\varphi_i(a)=\frac{d\varphi_i(x)}{dx}\bigg|_{x=a}=\frac{d\varphi_i(x)}{dx}\bigg|_{x=b}=0,$$

(5.3)

$$\psi_j(0)=\psi_j(b)=\frac{d^2\psi_j(y)}{dy^2}\bigg|_{y=0}=\frac{d^2\psi_j(y)}{dy^2}\bigg|_{y=b}=0.$$

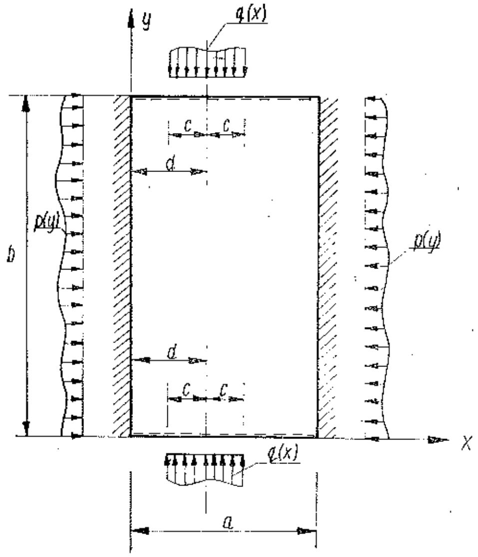

Fig. 8

The solution of the Eqs. (5.2) satisfying the boundary conditions (5.3) are the functions ([3], p. 766):

(5.4) $$\varphi_i(x)=\frac{\operatorname{ch}\vartheta_i\left(x-\frac{a}{2}\right)}{\operatorname{ch}\sigma_i}-\frac{\cos\vartheta_i\left(x-\frac{a}{2}\right)}{\cos\sigma_i},\qquad \psi_j(y)=\sin\beta_j y,$$

where

$$\sigma_1=2.365,\qquad \sigma_i=\vartheta_i\frac{a}{2}=\frac{4i-1}{4}\pi,\qquad i=1,3,5,7,\dots,$$

(5.5)

$$\beta_j=\frac{j\pi}{b},\qquad j=1,2,3,\dots.$$

Substituting the formulae (5.1) and (3.19) into the Eq. (4.1) and orthogonalizing the equation obtained with respect to the functions $\varphi_k(x)$, $\psi_l(y)$ we get the following infinite system of linear homogeneous algebraic equations (4.3) in which

(5.6) $$A_{klij}=D\left[\frac{ab}{2}(\vartheta_i^4+\beta_j^4)\,\delta_{ik}-2\vartheta_i^2\,\beta_j^2\,h_{klij}\right]\delta_{jl}-E_{klij},$$

where

$$E_{klij} = \vartheta_i^2 r_{klij} + 2\vartheta_i \beta_j s_{klij} - \beta_j^2 t_{klij},$$

$$h_{klij} = \int_0^a \int_0^b u_i(x)\varphi_k(x)\psi_j(y)\psi_l(y)\,dx\,dy,$$

(5.7)
$$r_{klij} = \int_0^a \int_0^b N_1(x,y)\,u_i(x)\varphi_k(x)\psi_j(y)\psi_l(y)\,dx\,dy,$$

$$s_{klij} = \int_0^a \int_0^b N_{12}(x,y)\,v_i(x)\varphi_k(x)g_j(y)\psi_l(y)\,dx\,dy,$$

$$t_{klij} = \int_0^a \int_0^b N_2(x,y)\,\varphi_i(x)\varphi_k(x)\psi_j(y)\psi_l(y)\,dxdy,$$

$$u_i(x) = \frac{\operatorname{ch}\vartheta_i\left(x-\frac{a}{2}\right)}{\operatorname{ch}\sigma_i} + \frac{\cos\vartheta_i\left(x-\frac{a}{2}\right)}{\cos\sigma_i},$$

(5.8)
$$v_i(x) = \frac{\operatorname{sh}\vartheta_i\left(x-\frac{a}{2}\right)}{\operatorname{ch}\sigma_i} + \frac{\sin\vartheta_i\left(x-\frac{a}{2}\right)}{\cos\sigma_i},$$

$$g_j(y) = \cos\beta_j y.$$

After integrating we obtain for $i \neq k$, $j \neq l$:

$$h_{klij} = 2ab\,\sigma_k^2 T_{ik}^{(1)},$$

$$r_{klij} = -2\nu b q_0 \sigma_k^2 T_{ik}^{(1)}\delta_{jl} - 2b \sum_{m=2,6,10,\dots}^{\infty} q_m \kappa_m S_m \left(\frac{\gamma_{j-l}^2}{\Delta_{m,j-l}} - \frac{\gamma_{j+l}^2}{\Delta_{m,j+l}}\right)\left[(\sigma_i+\sigma_k)T_{i+k,m}^{(2)} + (\sigma_i-\sigma_k)T_{i-k,m}^{(2)} + T_{k,i+m}^{(3)} + T_{k,i-m}^{(3)} + 2(\sigma_k+\eta_m)^2 T_{i,k+m}^{(4)} + 2(\sigma_k-\eta_m)^2 T_{i,k-m}^{(4)}\right],$$

(5.9)
$$s_{klij} = -2b \sum_{m=2,6,10,\dots}^{\infty} q_m \kappa_m^2 S_m \left(\frac{\gamma_{j-l}}{\Delta_{m,j-l}} - \frac{\gamma_{j+l}}{\Delta_{m,j+l}}\right)\left[\eta_m T_{i+k,m}^{(2)} + \eta_m T_{i-k,m}^{(2)} + T_{k,i+m}^{(3)} - T_{k,i-m}^{(3)} - 2\sigma_i(\sigma_i+\eta_m)T_{i,k+m}^{(4)} + 2\sigma_i(\sigma_i-\eta_m)T_{i,k-m}^{(4)}\right],$$

$$t_{klij} = 2b \sum_{m=2,6,10,\dots}^{\infty} q_m \kappa_m^3 S_m \left(\frac{1}{\Delta_{m,j-l}} - \frac{1}{\Delta_{m,j+l}}\right)\left[-(\sigma_i+\sigma_k)T_{i+k,m}^{(2)} - (\sigma_i-\sigma_k)T_{i-k,m}^{(2)} + T_{k,i+m}^{(3)} + T_{k,i-m}^{(3)} + 2\sigma_i^2 T_{i,k+m}^{(4)} + 2\sigma_k^2 T_{i,k-m}^{(4)}\right],$$

where

(5.10)
$$T^{(1)}_{i,k}=\frac{1}{(\sigma_i^4-\sigma_k^4)}(\sigma_i\operatorname{th}\sigma_i-\sigma_k\operatorname{th}\sigma_k),$$
$$T^{(2)}_{i\pm k,m}=\frac{\operatorname{th}\sigma_i\pm\operatorname{th}\sigma_k}{(\sigma_i\pm\sigma_k)^2+\eta_m^2},$$
$$T^{(3)}_{k,i\pm m}=\frac{\sigma_k\operatorname{th}\sigma_k-(\sigma_i\pm\eta_m)\operatorname{th}\sigma_i}{\sigma_k^2+(\sigma_i\pm\eta_m)^2},$$
$$T^{(4)}_{i,k\pm m}=\frac{\sigma_i\operatorname{th}\sigma_i-(\sigma_k\pm\eta_m)\operatorname{th}\sigma_k}{\sigma_i^4-(\sigma_k\pm\eta_m)^4},$$
$$S_m=\frac{\operatorname{sh}^2\kappa_m}{(2\kappa_m+\operatorname{sh}2\kappa_m)},$$

and

(5.11)
$$\eta_m=\alpha_m\frac{a}{2},\qquad \gamma_{j+l}=\gamma_j+\gamma_l,\qquad \gamma_r=\beta_r\frac{b}{2},\qquad r=j,\,l,$$
$$\Delta_{m,\,j\pm l}=(\kappa_m^2+\gamma_{j\pm l}^2)^2,\qquad j\pm l=2,4,6,\dots.$$

For $i=k$, $j=l$ we have

(5.12)
$$h_{klkl}=\frac{ab}{4}C_k,$$
$$r_{klkl}=-\nu\frac{b}{4}q_0C_k+256\gamma_l^2\sigma_k^3b\operatorname{th}\sigma_k\sum_{m=2,6,10,\dots}^{\infty}\frac{q_m\kappa_m}{\Delta^{(1)}_{ml}L_{km}}S_m,$$
$$s_{klkl}=-8\gamma_lb\operatorname{th}\sigma_k\sum_{m=2,6,10,\dots}^{\infty}\frac{q_m\kappa_m^2}{\Delta^{(1)}_{ml}}\left[\frac{2\eta_m^3}{L_{km}}+\frac{\sigma_k+\eta_m}{N_{k,k+m}}-\frac{\sigma_k-\eta_m}{N_{k,k-m}}\right]S_m,$$
$$t_{klkl}=-\frac{1}{2}q_0b+32b\gamma_l^2\operatorname{th}\sigma_k\sum_{m=2,6,10,\dots}^{\infty}\frac{q_m(\kappa_m^2+2\gamma_l^2)\eta_m}{\kappa_m\Delta^{(1)}_{ml}}\times$$
$$\times\left[\frac{1}{N_{k,k-m}}+\frac{4\sigma_k\eta_m}{L_{k,m}}-\frac{1}{N_{k,k+m}}\right]S_m,$$

where

(5.13)
$$\Delta^{(1)}_{ml}=(\kappa_m^2+4\gamma_l^2)^2,\qquad L_{k,m}=\sigma_k^4-\eta_m^4,$$
$$N_{k,k\pm m}=\sigma_k^2+(\sigma_k\pm\eta_m)^2,\qquad C_k=\frac{1}{\operatorname{ch}^2\sigma_k}-\frac{1}{\cos^2\sigma_k}+\frac{2\operatorname{th}\sigma_k}{\sigma_k}.$$

Introducing the formulae (5.9) and (5.12) into the Eqs. (5.6) we obtain for $i\neq k$, $j\neq l$:

(5.14)
$$A_{klij}=-16\sigma_i^2\sigma_k^2T^{(1)}_{ik}\left(4\gamma_l^2\frac{D}{a^2}-\frac{\nu\mu}{2a}q_0\right)\delta_{jl}-$$
$$-\frac{8}{b}\sum_{m=2,6,10,\dots}^{\infty}q_m\kappa_m^2S_m\left[\frac{H^{(1)}_{klijm}}{\Delta_{m,j-l}}-\frac{H^{(2)}_{klijm}}{\Delta_{m,j+l}}\right],$$

$$
(5.15)\quad
\begin{aligned}
H^{(1)}_{klijm} &= T^{(2)}_{i+k,\,m}\, e^{(1)}_{klijm} + T^{(2)}_{i-k,\,m}\, e^{(2)}_{klijm} + T^{(3)}_{k,\,i+m}\, f^{(1)}_{lijm} + \\
&\qquad + T^{(3)}_{k,\,i-m}\, f^{(2)}_{lijm} + 2T^{(4)}_{i,\,k+m}\, g^{(1)}_{klijm} + 2T^{(4)}_{i,\,k-m}\, g^{(2)}_{klijm},\\
H^{(2)}_{klijm} &= T^{(2)}_{i+k,\,m}\, e^{(3)}_{klijm} + T^{(2)}_{i-k,\,m}\, e^{(4)}_{klijm} + T^{(3)}_{k,\,i+m}\, f^{(3)}_{lijm} + \\
&\qquad + T^{(3)}_{k,\,i+m}\, f^{(4)}_{lijm} + 2T^{(4)}_{i,\,k+m}\, g^{(3)}_{klijm} + 2T^{(4)}_{i,\,k-m}\, g^{(4)}_{klijm},
\end{aligned}
$$

where

$$
(5.16)\quad
\begin{aligned}
e^{(1),(2)}_{klijm} &= (\sigma_i \pm \sigma_k)\,[\sigma_i^2\, \mu^2\, (\gamma_j - \gamma_l)^2 - \gamma_j^2\, \kappa_m^2] + 2\sigma_i\, \mu\, (\gamma_j - \gamma_l)\, \gamma_j\, \kappa_m\, \eta_m,\\
e^{(3),(4)}_{klijm} &= (\sigma_i \pm \sigma_k)\,[\sigma_i^2\, \mu^2\, (\gamma_j + \gamma_l)^2 - \gamma_j^2\, \kappa_m^2] + 2\sigma_i\, \mu\, (\gamma_j + \gamma_l)\, \gamma_j\, \kappa_m\, \eta_m;
\end{aligned}
$$

$$
(5.17)\quad
\begin{aligned}
f^{(1),(2)}_{lijm} &= [\sigma_i\, \mu\, (\gamma_j - \gamma_l) \pm \gamma_j\, \kappa_m]^2,\\
f^{(3),(4)}_{lijm} &= [\sigma_i\, \mu\, (\gamma_j + \gamma_l) \pm \gamma_j\, \kappa_m]^2;
\end{aligned}
$$

$$
(5.18)\quad
\begin{aligned}
g^{(1),(2)}_{klijm} &= [\mu\, (\gamma_j - \gamma_l)\, (\sigma_k \pm \eta_m) \mp \gamma_j\, \kappa_m]^2\, \sigma_i^2,\\
g^{(3),(4)}_{klijm} &= [\mu\, (\gamma_j + \gamma_l)\, (\sigma_k \pm \eta_m) \mp \gamma_j\, \kappa_m]^2\, \sigma_i^2.
\end{aligned}
$$

For $i=k$, $j=l$ we have

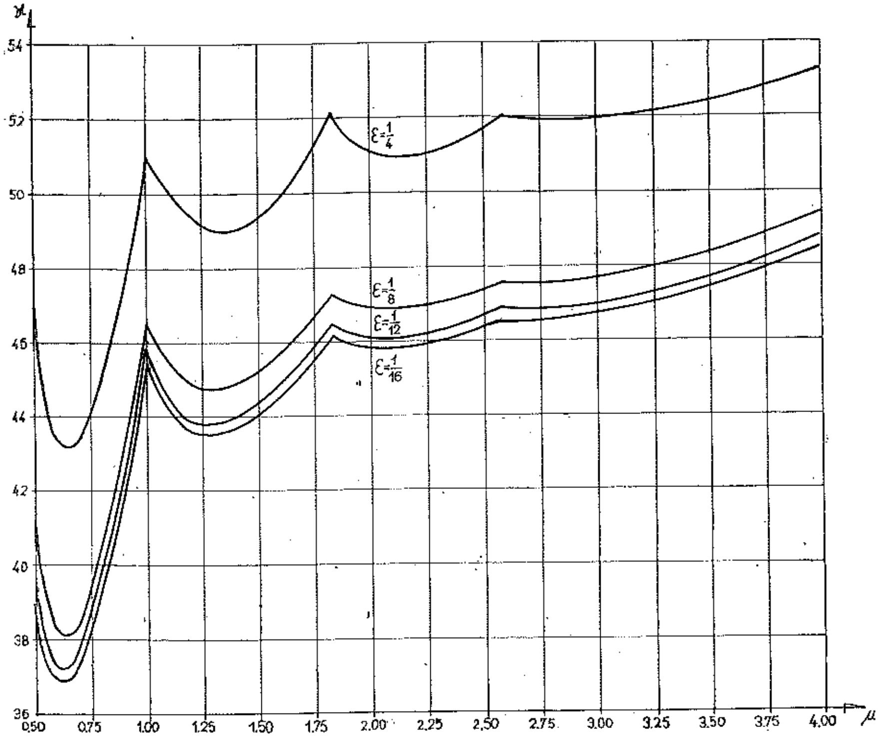

Fig. 9

$$
(5.19)\quad A_{klkl} = \frac{8}{a^2\,\mu}\, DK_{kl} + \nu\mu q_0\, \frac{1}{a}\, \sigma_k^2\, C_k - \frac{2a_0}{\mu a}\, \gamma_l^2 - \\
- 64\, \frac{\gamma_l^2}{b}\, \operatorname{th} \sigma_k \sum_{m=2,\,6,\,10,\,\ldots}^{\infty} \frac{q_m}{\kappa_m\, \Delta^{(1)}_{ml}}\, S_m\, G_{klm},
$$

Table 4. Values of coefficients 10 κ

ε \ μ	0.5	0.6	0.7	0.75	0.8	0.9	1.0	1.25	1.5	1.75	2.0	2.25	2.5	2.75	3.0	3.25	3.5	3.75	4.0
1/4	470	435	433	440	450	478	511	492	493	511	512	511	517	519	519	522	525	529	532
1/8	410	383	385	393	405	434	467	447	452	467	469	470	474	476	477	481	485	489	494
1/12	399	374	377	385	397	426	459	438	444	459	461	462	466	468	469	473	477	482	487
1/16	396	370	374	382	394	424	456	435	441	456	458	459	464	465	467	470	475	479	485
1/20	394	369	372	381	393	422	455	434	440	455	457	458	462	463	465	469	473	478	483
1/24	393	368	372	380	392	422	454	433	439	454	456	457	462	463	465	468	473	478	483
1/28	392	368	371	380	392	421	454	433	439	454	456	456	461	462	464	468	472	477	482

where

$$K_{kl}=\mu^2\sigma_k^4+\frac{1}{\mu^2}\gamma_l^4-\sigma_k^2\gamma_l^2 C_k,$$

(5.20)
$$G_{klm}=\frac{t^{(1)}_{k-m,\,l}}{N_{k,\,k-m}}-2\frac{t^{(2)}_{klm}}{L_{km}}+\frac{t^{(1)}_{k+m,\,l}}{N_{k,\,k+m}};$$

(5.21)
$$t^{(1)}_{k\pm m,\,l}=\sigma_k\kappa_m^3(\sigma_k\pm\eta_m)\mu-2\gamma_l^2(\kappa_m^2+2\gamma_l^2)\eta_m,$$
$$t_{klm}=\sigma_k(\sigma_k^4\kappa_m^2\mu^2+\kappa_m^3\eta_m^3\mu-4\gamma_l^2\eta_m^2\kappa_m^2-8\eta_m^2\gamma_l^4).$$

The infinite system of the Eqs. (4.3) the matrix elements of which are determined by means of the formulae (5.14) and (5.19) is composed in the same way as those in the previous section, of two idependent systems. The first system contains the indices $i, k=1, 3, 5, \ldots, j, l=1, 3, 5, \ldots$, and the second system contains the indices $i, k=1, 3, 5, \ldots, j, l=2, 4, 6, \ldots$.

The numerical values of the coefficients κ computed from the Eqs. (4.6) corresponding to the numbers 4, 8 and 12 of equations in the system (4.3) differ very slightly. The largest discrepancy does not exceed 0.04%.

The coefficients κ computed for the consecutive values of ε and μ on the basis of the Eq. (4.6) with the use of the formulae (5.14), (5.19) and (3.20) are put in the Table 4. The corresponding diagrams facilitating the application of the results of calculations are shown in Fig. 9.

Acknowledgement

This work was prepared on the ground of my doctor's thesis carried out under the guidance of Prof. Dr. Z. Mazurkiewicz to whom I owe my cordial thanks for his very valuable instructions and remarks.

References

1. Z. Mazurkiewicz, A. Wiweger, *Static and dynamic problems of elastic shells of small rise*, Arch. Mech. Stos., **20**, 2, 1968.
2. Z. Kączkowski, *Płyty*, Arkady, Warszawa 1967.
3. W. Nowacki, *Mechanika budowli*, t. 2, PWN, Warszawa 1967.
4. W. Nowacki, *Mechanika budowli*, t. 3, PWN, Warszawa 1966.
5. W. Nowacki, *Z zagadnień stateczności płyt prostokątnych*, Zakł. Mech. Bud. P. Gd. (odbitka z maszynopisu).
6. P. Lardy, *Sur une méthode nouvelle de resolution du problème des delles rectangulaires encastre'es*, Mémoires de A.I.P.Ch., vol. 13, Zurich 1953.
7. A. Sommerfeld, *Über die Knicksicherheit der Stege von Wälzprofilen*, Z. f. Math. u. Phys., **54**, 1906.
8. M. T. Huber, *Pisma*, t. 2, PWN, Warszawa 1956.
9. S. P. Timoshenko, J. M. Gere, *Teoria stateczności sprężystej*, (tłum. z wyd. II), Arkady, Warszawa 1962.
10. S. P. Timoshenko, S. Wojnowsky-Krieger, *Teoria płyt i powłok*, (tłum. z wyd. II), Arkady, Warszawa 1962.
11. A. S. Wolmir, *Ustojcziwost deformirujemych sistem*, Nauka, Moskwa 1967.

12. A. Pflüger, *Stabilitätsprobleme der Elastostatik*, Springer-Verlag, Berlin-Göttingen Heidelberg-New York 1964.
13. N. Yamaki, *The Reports of the Institute of High Speed Mechanics*, Tohoku University, Sendai, Japan, **3**, 1953; **4**, 1954; **5**, 1955.
14. J. H. Wilkinson, *The algebraic eigenvalue problem*, Clarendon Press, Oxford 1965.
15. W. N. Faddiejewa, *Metody numeryczne algebry liniowej* (tłum. z ros.), PWN, Warszawa 1955.
16. I. M. Ryžyk, I. S. Gradsztejn, *Tablice całek, sum, szeregów i iloczynów* (tłum. z wyd. III), PWN, Warszawa 1964.

Streszczenie

WYBOCZENIE PŁYT PROSTOKĄTNYCH POD WPŁYWEM OBCIĄŻENIA NIECIĄGŁEGO WZDŁUŻ BRZEGÓW

Przedmiotem pracy jest problem wyboczenia sprężystego płyt prostokątnych, izotropowych, sprężyście jednorodnych, o małych grubościach, obciążonych dowolnie wzdłuż brzegów, przy różnych warunkach brzegowych. Przedstawione rozwiązanie obejmuje dwa etapy, tj. wyznaczenie rozkładów sił wewnętrznych w tarczy poddanej działaniu dowolnego obciążenja nieciągłego oraz obliczenie parametrów krytycznych, powodujących wyboczenie płyty. W pierwszym etapie zastosowano skończoną transformację Fouriera, w drugim podwójne szeregi Fouriera i metodę P. Lardy'ego do rozwiązania problemu wyboczenia płyty w dwóch przypadkach warunków brzegowych, tj. swobodnie podpartej na całym obwodzie oraz utwierdzonej wzdłuż dwóch przeciwległych krawędzi i swobodnie podpartej na pozostałych brzegach. W obu rozważanych przypadkach rozwiązanie problemu doprowadzono do nieskończonych układów algebraicznych, liniowych równań jednorodnych. Wyniki obliczeń zestawiono w tablicach oraz na ich podstawie sporządzono wykresy.

Резюме

ПРОДОЛЬНЫЙ ИЗГИБ ПРЯМОУГОЛЬНЫХ ПЛИТ ПОД ВЛИЯНИЕМ РАЗРЫВНОЙ НАГРУЗКИ ВДОЛЬ КРАЕВ

Предметом работы является проблема упругого продольного изгиба изотропных, упруго однородных, малой толщины, прямоугольных плит нагруженных вдоль краев при разных граничных условиях. Представленное решение охватывает два этапа т.е. определение распределений внутренних сил в диске подвергнутом действию произвольной разрывной нагрузки и вычисление критических параметров, вызывающих продольный изгиб плиты. В первом этапе применено конечное преобразование Фурье, во втором двойные ряды Фурье и метод П. Ларди для решения проблемы продольного изгиба плиты в двух случаях граничных условий т.е. свободно подпертой на целом периметре, а также закрепленной дволь двух противолежащих краев и свободно подпертой на остальных краях. В обоих обсуждаемых случаях решение проблемы сведено к бесконечным системам алгебраических, линейных однородных уравнений. Результаты вычислений составлены в таблицах и на их основе построены графики.

WYŻSZA SZKOŁA INŻYNIERSKA W LUBLINIE

Received April 9, 1975.